VIBRATION ENERGY HARVESTING FROM THE UNSPRUNG SUSPENSION OF A VEHICLE FOR ASSET MONITORING USING AN ELECTROMAGNETIC TRANSDUCER

A.C. Waterbury[1], S.D. Lin[1], and P.K. Wright[1]
[1]Mechanical Engineering Department, University of California, Berkeley, Berkeley, CA, USA

Abstract: A potential energy source for powering wireless nodes for asset monitoring of shipping fleets or large equipment is the vibrational energy associated with the suspensions of the vehicles. The acceleration of the unsprung suspension of a passenger vehicle was recorded during trips in California. The acceleration data revealed that the vibrational energy was consistently concentrated below 30 Hz. The recorded acceleration data was simulated on a vibration table and harvested with an electromagnetic transducer configured to resonate at 20 Hz. The average induced power ranged from about 30–600 μW and seemed to depend on the road surface.

Keywords: Vibration Energy Harvesting, Electromagnetic, Vehicle Suspension

INTRODUCTION

Monitoring large fleets of vehicles can be implemented using wireless nodes, and vibrations from normal vehicle operation are one potential harvestable energy sources that can power such nodes. Wireless nodes provide a low infrastructure retrofit to existing systems and can have functional lifetimes extending to decades when implemented with energy harvesting solutions [1].

A variety of vibration sources within a passenger vehicle were surveyed. Vibrations associated with the dashboard, firewall, engine, and unsprung suspension of a passenger vehicle were characterized. The largest magnitude vibrations were associated with the unsprung vehicle suspension.

Traditional vibration energy harvesting involves an inertial system where the resonant frequency matches the frequency of the vibration to be harvested. Piezoelectric, electrostatic, and electromagnetic transduction mechanisms and designs have been widely researched over the past decade or more.

In the case of vehicle tracking, low power radios are not viable because of the distributed and dynamic nature of the nodes. As such, nodes would communicate through cellular networks with radio transmission powers approaching one watt. GPS receivers are also a relatively high power sensor. Using one watt as the rough active power, a harvester would need to generate one milliwatt to maintain a duty cycle of 0.1%, enabling regular condition monitoring communication. As a result of the large power requirement and the harsh nature of the target environment, electromagnetic transduction became attractive because the large inertial mass enabled traditional coil windings to be implemented. Additionally, electromagnetic transduction allowed greater freedom in designing spring structures to withstand the shock loads of uneven road surfaces.

This paper briefly characterizes the vibrations associated with an unsprung vehicle suspension, and presents the results from using the measured vibration data to excite a vibration harvester with a vibration table. The design of the vibration harvester is also briefly discussed.

UNSPRUNG SUSPENSION VIBRATIONS

The vibrations associated with unsprung vehicle suspensions are the loads of road features transmitted through the tire and wheel. During data collection a wireless accelerometer was clamped to the control arm at the wheel upright.

The passenger car completed the two trips shown in Figure 1. GPS information and vibration data from the accelerometers were surveyed every three minutes during the trips. At each survey point, the accelerometer data was recorded for 2.5 seconds at a sample rate of 2 kHz.

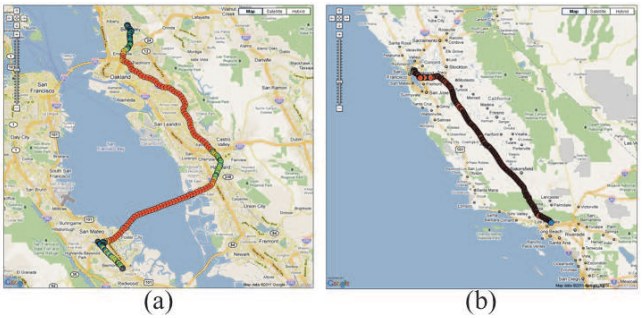

(a) (b)

Fig. 1: (a) Trip from San Mateo to Berkeley California. (b) Trip from Berkeley to Los Angeles California. Dots represent survey locations.

The trip shown in Figure 1a had 164 survey points,

and the trip in Figure 1b had 769 survey points.

The axis normal to the road surface contained the vibrations of the greatest magnitude. The vibrational energy was almost universally below 100 Hz, and the highest acceleration peaks were consistently densely concentrated below 30 Hz as Figure 2 indicates.

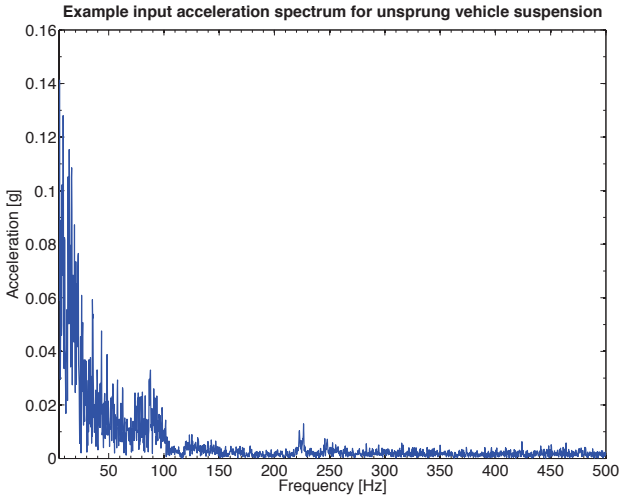

Fig. 2: Representative acceleration spectrum for the unsprung suspension of a passenger vehicle

VIBRATION HARVESTER

Vibration harvesters based on coreless motor architectures have previously been investigated in [2]. The harvester used in this study had a speaker motor architecture with a single air gap in the magnetic flux path defined by a steel low reluctance magnetic circuit, as shown in Figure 3, that also acts as the proof mass of the inertial system. Interchangeable planar multiturn stainless steel springs above and below the proof mass allow the resonant frequency to be modified. Installing springs of the appropriate thickness allowed the harvester to be configured to resonate in the range of 20–120 Hz. Table 1 provides physical details for the prototype harvester.

Table 1: Prototype harvester physical parameters

# of coil turns, N	660
Mass of resonant system, m [kg]	0.027
Coil resistance, R_c [Ω]	76
Self-inductance, L [mH]	50
Simulated average flux density, B, [T]	0.25
Average length of a coil turn, l, [mm]	25.4
Maximum translation amplitude [mm]	2.5
Overall harvester volume [cm^3]	18.0
Configurable resonant freq. range [Hz]	20–120
Linear resonant range [Hz]	90–120

The adaptable resonant frequency came at the expense of an optimized design for a specific target, but it provided the freedom to evaluate performance for selected parts of the acceleration frequency spectrum. The large translation amplitudes at lower resonant frequencies caused an unanticipated nonlinear spring hardening to arise. For resonant frequencies below 90 Hz, the nonlinearity was present, effectively stroke limiting the device. Significantly less power was generated due to the stoke limiting than would be expected from a similar harvester with linear behavior. The stroke limiting also caused the optimum electrical load to decrease. The smaller optimum load increased the transduction force, reducing the destructive behavior of the hardening on the motion of the inertial mass.

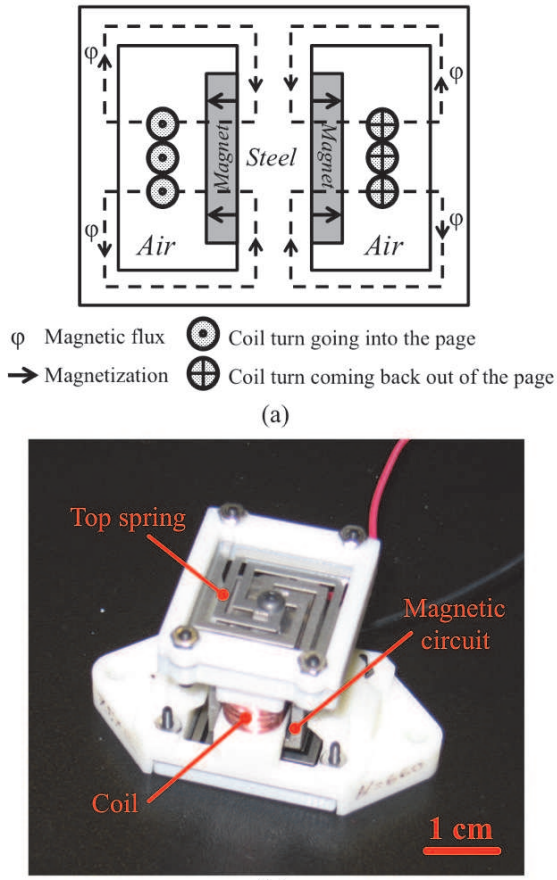

Fig. 3: (a) Cross section illustration of the prototype harvester magnetic circuit. (b) Prototype harvester

When the springs remain linear, the harvester can be modeled as a mass–spring–damper system with an additional transduction force. The transduction force is a Lorentz force that is proportional to the induced current, i, the magnet flux density, B, the number of coil turns, N, and the length of the conductor in the magnetic field, l. The transduction force is often

transformed into additional damping if the electrical load is purely resistive and the self–inductance can be ignored [3]. The general equation of motion for the prototype harvester is

$$\ddot{z} + 2\omega_0\zeta\dot{z} + {\omega_0}^2 z + \frac{1}{m}NBli = \ddot{y}, \quad (1)$$

where z is the relative position of the inertial mass and the base or frame of the device. The position of the base is represented by y. The resonant frequency of the device is given by ω_0, and the parasitic damping is given by ζ. Finally, m is the inertial mass. A damping ratio of 0.0006 was back calculated from open circuit ring-down tests. Thus, the system had a very high mechanical Q of about 830.

The equation for the induced voltage, V, of the prototype harvester with a resistive load is given by

$$V = i(R_c + R_l) + L\frac{di}{dt} + NBl\frac{dz}{dt}, \quad (2)$$

where R_c and R_l are the resistance of the coil and the load, respectively. The self–inductance is represented by L. The full set of differential equations providing a general description of the coupled mechanical and electrical domains is

$$\frac{d}{dt}\begin{bmatrix} z \\ v_z \\ i \end{bmatrix} = \begin{bmatrix} 0 \\ \ddot{y} \\ 0 \end{bmatrix} - \begin{bmatrix} 0 & -1 & 0 \\ {\omega_0}^2 & 2\omega_0\zeta & -\frac{NBl}{m} \\ 0 & \frac{NBl}{L} & \frac{R_c+R_l}{L} \end{bmatrix}\begin{bmatrix} z \\ v_z \\ i \end{bmatrix}, \quad (3)$$

where v_z is the relative velocity of the inertial mass.

EXPERIMENTS

Experimental setup

The vibration platform shown in Figure 4 was used to simulate the acceleration data collected during the two driving trips in California.

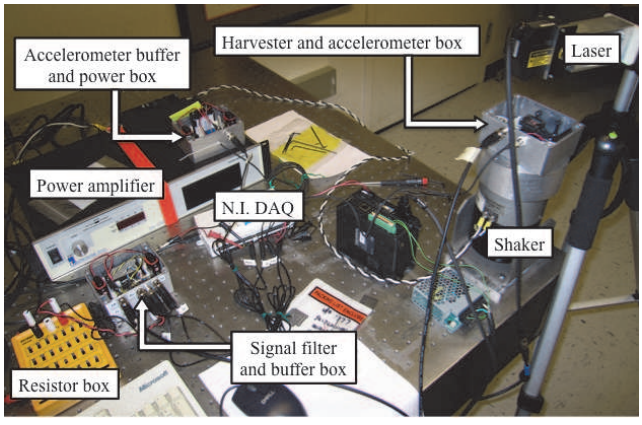

Fig. 4: Vibration platform components

The 2.5 seconds of acceleration data in each set was reproduced on the vibration platform. Data sets that caused the vibration platform to hit its limit stops were not included due to the resulting phantom impulses.

The setup measured the induced voltage, current, acceleration, and the position of the inertial mass. A Labview program sequentially sent acceleration data sets to the shaker with a 30 second pause between data sets. The program simultaneously recorded the corresponding induced harvester performance.

Harvester configuration

The consistently dense cluster of vibration peaks below 30 Hz was targeted as the region to attempt to harvest. The harvester was configured with 0.13 mm thick springs, causing it to resonate at 20 Hz. The very low resonant frequency resulted in the device being stroke limited by the spring hardening nonlinearity and the maximum translation amplitude of 2.5 mm.

The optimum electrical load was determined from a load sweep at 20 Hz with an input acceleration amplitude of 0.1 g. The optimum load was 100 Ω.

To further illustrate that lower frequency vibrations should be targeted for this application, the harvester was configured to resonate at 93 Hz. This frequency was selected because region between 90–100 Hz often contained a cluster of peaks, albeit significantly smaller than the peaks below 30 Hz. When configured to resonate at 93 Hz, the optimum electrical load was 310 Ω and was determined from a load sweep at 0.1 g.

Results

The large number of data sets encompassed typical operating conditions of a vehicle and provided a statistical significance to the results. Despite using a resonant harvester on a system with an ever-changing input acceleration spectrum, significant power was induced. Table 2 summarizes the harvesting results for the two trips.

The results for the trip from San Mateo to Berkeley showed that significant power could be generated, approaching the level of 1 mW that was roughly specified. However, the power numbers from the trip from Berkeley to Los Angeles (LA) provide a stark contrast. The difference in induced power between the two trips was likely the result of smoother road surfaces.

Comparing the results from the 20 Hz and 93 Hz resonant frequency configurations for trip from Berkeley to LA indicates that targeting vibrations below 30 Hz significantly improved the power that was harvested.

The induced voltages were all low for rectification.

Figure 5 shows an induced voltage waveform for the trip from San Mateo to Berkeley that is representative of the mean power harvested in the 97+ kph category for that trip.

Table 2: Energy harvesting results for the two trips

Speed [kph]	Voltage [Vrms]		Power [µW]		Max. pwr. [µW]
	Mean	SD	Mean	SD	
San Mateo to Berkeley, resonant frequency: 20 Hz					
0-48	0.071	0.074	104	181	824
48-97	0.191	0.064	399	267	964
97+	0.228	0.078	574	343	1290
Berkeley to LA, resonant frequency: 20 Hz					
0-48	0.039	0.042	32	79	534
48-97	0.062	0.034	50	57	361
97+	0.061	0.038	51	76	788
Berkeley to LA, resonant frequency: 93 Hz					
0-48	0.010	0.014	1	4	32
48-97	0.022	0.015	2	4	27
97+	0.023	0.016	3	5	62

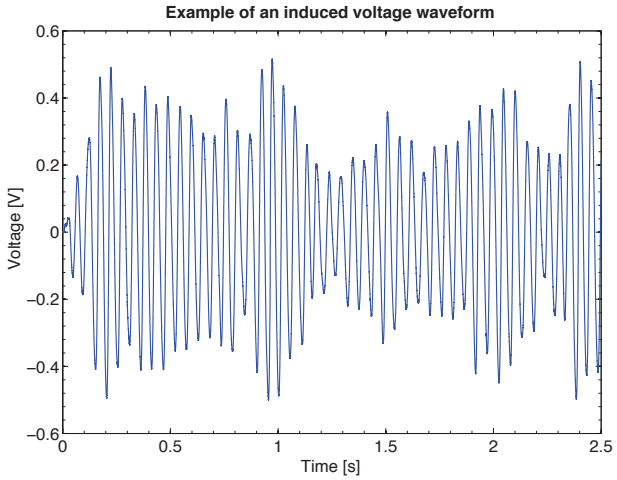

Fig. 5: Induced voltage waveform representative of the mean power harvested in the 97+ kph category of the trip from San Mateo to Berkeley.

CONCLUSIONS

The vibration energy associated with an unsprung vehicle suspension that should be target by vibration energy harvesters is densely clustered below 30 Hz. With the prototype harvester configured to resonate at 20 Hz, the induced power ranged from roughly 30–600 µW for the two trips in California. Despite the somewhat low induced power, the results were still encouraging considering the unoptimized harvester design and the stroke limited behavior. The stroke limiting and corresponding lower optimal electrical loads also contributed to the magnitude of the induced voltages being too low to be easily rectified. While voltages below one volt have been rectified, there are significant losses [4]. Thus, harvester designs in this space should be optimized for resonant frequencies below 30 Hz and emphasize improved induced voltages.

The results from the two trips also suggest that vibration energy harvesting performance for unsprung vehicle suspensions is dependent on parameters such as road surface, tire profile, and traveling speed.

ACKNOWLEDGEMENTS

The authors would like to thank Dan Steingart and Andrew Pullin for providing the acceleration data sets used in this work.

The authors also thank the California Energy Commission for supporting this research under contract 500-01-43.

REFERENCES

[1] Roundy S, Wright P, Rabaey J. Energy scavenging for wireless sensor networks with special focus on vibrations. Norwell, MA: Kluwer academic publishers; 2004. p. 3–4.

[2] Beeby SP, Torah RN, Tudor MJ, Glynne-Jones P, O'Donnell T, Saha CR, et al. A micro electromagnetic generator for vibration energy harvesting. *Journal of Micromechanics and Microengineering*. 2007 Jun. 5; 17(7): 1257–65.

[3] Williams CB, Yates RB. Analysis of a micro-electric generator for microsystems. *Sensors and Actuators A: Physical*. 1996 Mar.; 52(1-3): 8–11.

[4] Seeman MD, Sanders SR, Rabaey JM. An ultra-low-power power management IC for energy-scavenged Wireless Sensor Nodes. *Proceedings of the 2008 Power Electronics Specialists Conference (PESC 2008)*, IEEE. Rhodes, Greece; 2008. p. 925–31.